
ACOUSTIC CHARACTERIZATION OF SPEECH RHYTHM: GOING BEYOND METRICS WITH RECURRENT NEURAL NETWORKS

François Deloche^{1, 2, *}, Laurent Bonnasse-Gahot³, and Judit Gervain^{4, 5, 6}

¹Department of Speech, Language, and Hearing Sciences, Purdue University, West Lafayette, USA

²Hearing Technology Lab, Department of Information Technology, Ghent University, Ghent, Belgium

³Centre d'Analyse et de Mathématiques Sociales, CNRS, EHESS, Paris, France

⁴Integrative Neuroscience and Cognition Center, CNRS & Université Paris Cité, Paris, France

⁵Department of Developmental and Social Psychology, University of Padua, Padua, Italy

⁶Padova Neuroscience Center, University of Padua, Padua, Italy

*e-mail: francois.deloche@polytechnique.org

ABSTRACT

Languages have long been described according to their perceived rhythmic attributes. The associated typologies are of interest in psycholinguistics as they partly predict newborns' abilities to discriminate between languages and provide insights into how adult listeners process non-native languages. Despite the relative success of rhythm metrics in supporting the existence of linguistic rhythmic classes, quantitative studies have yet to capture the full complexity of temporal regularities associated with speech rhythm. We argue that deep learning offers a powerful pattern-recognition approach to advance the characterization of the acoustic bases of speech rhythm. To explore this hypothesis, we trained a medium-sized recurrent neural network on a language identification task over a large database of speech recordings in 21 languages. The network had access to the amplitude envelopes and a variable identifying the voiced segments, assuming that this signal would poorly convey phonetic information but preserve prosodic features. The network was able to identify the language of 10-second recordings in 40% of the cases, and the language was in the top-3 guesses in two-thirds of the cases. Visualization methods show that representations built from the network activations are consistent with speech rhythm typologies, although the resulting maps are more complex than two separated clusters between stress and syllable-timed languages. We further analyzed the model by identifying correlations between network activations and known speech rhythm metrics. The findings illustrate the potential of deep learning tools to advance our understanding of speech rhythm through the identification and exploration of linguistically relevant acoustic feature spaces.

1 Introduction

When listening to different languages, even ones we do not know or understand, we often have the impression that some languages, like Spanish and Italian, have similar rhythms, while others, like Japanese and English, are quite distinct in their rhythmicity. The percept of linguistic rhythm is so powerful that newborn infants can rely on it to distinguish rhythmically different languages [Nazzi et al., 1998, Mehler et al., 2000], and adults use the rhythmic template of their native language when listening to foreign languages [Cutler, 1994]. Yet, the acoustic correlates of linguistic rhythm in the speech signal are only partially understood. Theories of speech rhythm originally relied on the isochrony principle, which holds that speech is organized into units of equal duration [Pike, 1945, Abercrombie, 1967]. A dichotomy between 'syllable-timed' and 'stress-timed' languages was postulated, depending on whether the isochronous units were believed to be the syllables or the intervals between stressed syllables. The isochrony principle turned out not to be supported by empirical evidence [Roach, 1982, Dauer, 1983] and it is now discarded, but the term 'speech rhythm' and the associated typology of languages have remained in use. Despite the absence of isochronous units, the systematic alternations of strong and weak elements at different levels of the phonological hierarchy gives rise to a sense of rhythm [Langus et al., 2017]. At the physical level, several dimensions are involved and contribute to the perception of prominence, mainly intensity, duration, pitch,

and vowel quality [Terken and Hermes, 2000]. Research on speech rhythm has thus moved from the search of simple isochronous patterns to the more challenging task of characterizing potentially weaker regularities affecting a larger number of dimensions [Bertinetto, 1989, Kohler, 2009a, Cumming and Nolan, 2010, Turk and Shattuck-Hufnagel, 2013]. One fruitful approach, originally proposed by Dauer [Dauer, 1983], has been to highlight correlations between the rhythmic classes and several phonological differences between languages, such as the complexity of syllable structure or the presence of reduced vowels. This description motivated the development of speech rhythm metrics defined by summary statistics on the duration of consonantal or vocalic intervals [Ramus et al., 1999, Grabe and Low, 2002], which were among the first studies to provide quantitative evidence for the existence of rhythmic classes. These studies also coincided with a renewed interest in speech rhythm within the psycholinguistics community, following the observation that newborns can discriminate between languages belonging to different rhythmic classes [Moon et al., 1993, Nazzi et al., 1998, Mehler et al., 2000], even if those languages were unfamiliar to them, i.e. not spoken by their mothers during pregnancy. This ability allows newborn infants to discover that there are multiple languages in their environments, if they are born multilingual between rhythmically different languages [Gervain and Mehler, 2010]. Similarly, adults have been shown to rely on the rhythm of their native language even when listening to foreign languages [Cutler, 1994]. Developing a more quantitative foundation for speech rhythm is also a goal in applied areas like Computer Assisted Language Learning, where it could for example enhance the assessment of non-native speakers’ oral proficiency [Kyriakopoulos et al., 2019].

Despite the relative success of speech rhythm metrics in separating prototypical syllable- and stress-timed languages, they have been criticized for being unreliable, since variations induced by speech rate, speaker identity or speech corpus within the same language can exceed cross-linguistic variation [Arvaniti, 2009, Wiget et al., 2010, Arvaniti, 2012]. Some authors even argue that research based on rhythm metrics has reached its limit [Rathcke and Smith, 2015] and has not sufficiently characterized the timing regularities of speech [Arvaniti, 2009].

These shortcomings call for new tools to revisit the acoustic bases of speech rhythm. These tools, as we argue in this paper, could come from the field of deep learning. This approach aligns well with a trend that has emerged over the last decade in cognitive science, characterized by the increasing use of deep neural networks (DNNs) in the study of sensory systems and perception [Yamins and DiCarlo, 2016, Kell and McDermott, 2019, Storrs and Kriegeskorte, 2019].

DNNs are compositional models made of successive layers of linear and non-linear transformations. They contain a large number of variables that define the ‘synaptic’ weights of the model units called artificial neurons. When a DNN is trained on a large database of examples, it can learn a complex non-linear relationship between input data and outputs (labels) [LeCun et al., 2015]. DNN models trained in a supervised fashion can achieve human-level performance on tasks that individuals perform in their everyday environment such as visual object recognition [Krizhevsky et al., 2017] or speech recognition [Yu and Deng, 2015].

To test whether a deep learning model could provide insights into cross-linguistic aspects of speech rhythm, we trained a recurrent neural network with long short-term memory (LSTM) units [Hochreiter and Schmidhuber, 1997] on a language identification task involving typologically and genetically different languages. The network was only given three features from the speech recordings to constrain the network to rely on speech rhythm: two amplitude envelopes – one derived from the raw waveforms and one from a high-passed version of the waveforms – and a variable identifying the voiced segments. Our assumption is that these features convey phonetic information poorly, but preserve the information related to rhythm, such as the alternation of weak and strong segments and the consonant-vowel segmentation. The network was trained on a large dataset of speech recordings in 21 languages collected from several open web databases. Our main question is whether the internal representation of the trained model is consistent with the rhythmic typology of languages. To this end, we analyzed the network error structure, and we used several visualization methods to build language maps from network output activations. We obtained successful language identification in 40% of the cases, and the target language was in the top 3 guesses in two-thirds of the cases. We also found that linear combinations of a sub-set of these activations presented strong correlation with established speech rhythm metrics, allowing interpretations in line with previous work. The findings illustrate the strong potential of deep learning methods for speech rhythm research, providing a tool to strengthen the connection between hypotheses on the perception of language, and underlying statistical regularities present in the speech signal, even when these regularities are not easily quantified by more classical analytical models.

2 Methods

2.1 Speech data

The DNN model’s task was to identify the language of 10-second speech recordings from 21 languages. To this end, a very large dataset was assembled by retrieving speech recordings from five open web databases. The main database was the Common Voice dataset, an open source collaborative project launched by Mozilla in 2017 collecting sentences read by web users [Ardila et al., 2020], representing 66% of the recordings. The other databases were LibriVox (14.5% of the recordings), a collaborative project for the creation of public domain audiobooks; a set of radio podcasts listed by the Wide

Language Index for the Great Language Game (WLI - 14.5%) [Skirgård et al., 2017]; VoxForge, a collaborative project similar to the Common Voice initiative (4%); and Tatoeba, another collaborative database of read example sentences (1%). The entire dataset represents a large variety of speakers (25,000 in total) and recording settings, a necessary condition for the neural network to generalize to examples outside the training set. The data also includes different elicitation methods (reading of short sentences, reading of running text, connected speech) although the reading of disconnected sentences is the main elicitation method represented. The data was cleaned in several ways before being used to train the model. Files that excessively contained music excerpts in the LibriVox audiobooks and the WLI podcasts were removed. For Common Voice, the metadata was used to exclude the recordings of the lowest quality, based on down- and up-votes as well as speech by non-native speakers, based on the ‘accent’ field. We also chose not to include speakers with particular accents, especially French Canadian speakers for French. However, we applied this process only to a limited extent, as we could not separate all regional varieties within a language due to lacking labels in the Common Voice metadata, e.g. European Portuguese and Brazilian Portuguese, even though they are known to exhibit different rhythmic characteristics. To create 10-second-long segments, files from the same speaker were concatenated together with a 0.3-sec pause between each file, if they were shorter than 10 seconds, whereas longer recordings (typically from Librivox and the WLI) were split into 10-sec segments. We chose a relatively long segment duration to allow the neural network to adapt to recording settings and to accumulate evidence over several sentences. The resulting dataset contained 440,000 10-sec recording segments in total, representing 1,200 hours of speech data. The recording segments, however, were not evenly distributed across languages (Table 1). The two most represented languages, German and English, accounted for 30% of the dataset. On the other end of the list, Estonian, Japanese and Hungarian only have 3 000–4 000 segments (<1%). This major bias in favor of the most widespread languages was counterbalanced by adding weights to the cost function during model training, as specified further on.

2.2 Model inputs

Inputs extracted from the speech recordings were intentionally limited to force the model to rely primarily on prosodic cues. The inputs consisted of a three-dimensional feature vector presented at a sampling rate of 31.25 Hz. This sampling rate corresponds to time windows of 512 samples at 16 kHz, or 32 ms. The first two features were the average sound pressure level (SPL) and the SPL level with a pre-emphasis on high frequencies (SPL-H), both in dB, computed on the 32-ms time windows. The third feature was a variable indicating whether the windows belonged to voiced segments (0 for voiceless segments, 1 otherwise). They are illustrated on an example in Fig. 1.

We chose these features on the basis of acoustic studies of prominence in Swedish [Fant et al., 2000]. Specifically, the amplitude envelopes SPL and SPL-H delineate the main prosodic boundaries and syllable contours. The local alternations between low and high intensity segments provide additional clues about consonant-vowel (CV) transitions. These transitions are further indicated by the addition of SPL-H, since most vowels and consonants have a different balance between low and high frequencies; for example, most fricatives primarily carry energy in the higher frequency range. Variations in intensity can also be an indication of syllable prominence. The difference between SPL-H and SPL also provides information about spectral tilt, which in turn is a correlate of vowel openness, vowel quality and stress [Sluijter and Van Heuven, 1996, Fant et al., 2000]. The third feature naturally marks the transitions between voiced and unvoiced segments. The sampling frequency (31.25 Hz) was chosen so that the corresponding Nyquist frequency was of the same order as the rate of 10-15 phonemes per second in normal speech.

Prior to the computation of the intensity measures (SPL and SPL-H), the signal amplitude of each recording was normalized to ensure that the dynamic ranges of all recordings were comparable. SPL-H is the intensity of the signal after passing through a gentle high-pass filter with the following frequency response:

$$H(j\omega) = \frac{1 + j\omega/\omega_A}{1 + j\omega/\omega_B},$$

or, after applying the bilinear transform:

$$H(z) = \frac{(1 + A) + (1 - A)z^{-1}}{(1 + B) + (1 - B)z^{-1}},$$

with $A = (2/\omega_A)f_s$, $B = (2/\omega_B)f_s$, $\omega_A = 2\pi \times 200$ Hz, $\omega_B = 2\pi \times 5000$ Hz, and f_s the sampling frequency (16 kHz). This filter applies an extra gain of around +20dB for frequencies above 1 kHz (see figure 12 in [Fant et al., 2000] considering the same filter). To compute the third feature (voicing information), we used the Parselmouth library based on Praat to estimate the time course of the fundamental frequency F0 [Jadoul et al., 2018, Boersma and Weenink, 2018]. As a result, our code provides the option to include F0 as the third feature (Fig. 1), however we only kept the voicing information in the main version of the model presented in the Results section; i.e., voiceless segments are coded as 0, other

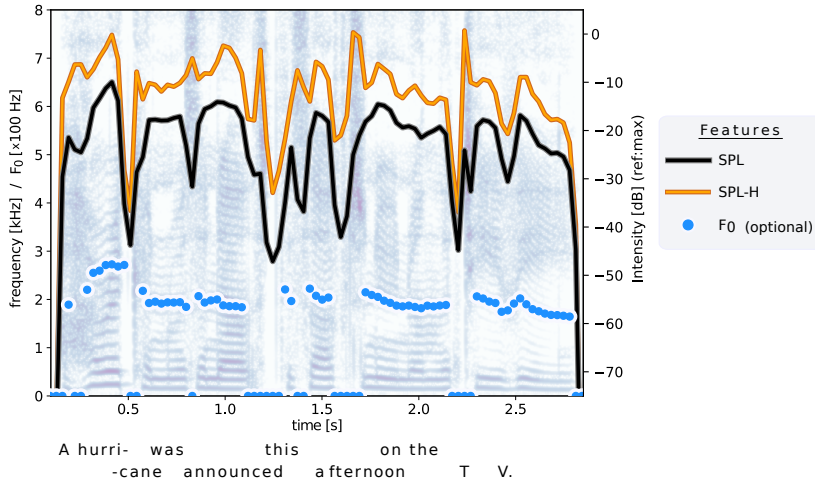


Figure 1: Features for the language identification task illustrated on the sentence: ‘a hurricane was announced this afternoon on the TV’ (from the Ramus corpus [Ramus et al., 1999]). SPL: Sound pressure level. SPL-H: Sound pressure level after the signal is passed through a gentle high-pass filter. F0 : the fundamental frequency. In the main version of the model presented in the paper, only the voicing information is kept for the third dimension – 1 for voiced segments ($F_0 \neq 0$); 0 for voiceless segments ($F_0 = 0$). The three features are sampled at 31.25 Hz. The spectrogram of the sentence is shown for guidance (background image).

segments are set to 1 irrespective of the F0 value. Training the neural network was more difficult when F0 was included instead of the voicing information, especially for the models with a small number of units that were in general preferred (see next subsection). Before being processed by the DNN, the features were normalized by applying a constant affine transformation to each dimension so that each input was in the range [0,1].

Language	Nb files	Language	Nb files	Language	Nb files
German	72,368 (16.3%)	Russian	14,880 (3.3%)	Polish *	6,832 (1.5%)
English *	64,512 (14.5%)	Mandarin	14,000 (3.1%)	Danish	6,048 (1.4%)
French *	54,816 (12.3%)	Portuguese	14,112 (3.2%)	Arabic	5,520 (1.2%)
Catalan *	46,576 (10.5%)	Korean	10,896 (2.4%)	Turkish	5,376 (1.2%)
Spanish *	43,584 (9.8%)	Swedish	10,320 (2.3%)	Estonian	3,520 (0.8%)
Italian *	30,416 (6.8%)	Dutch *	10,640 (2.4%)	Japanese *	3,856 (0.9%)
Basque	15,600 (3.5%)	Finnish	8,320 (1.9%)	Hungarian	3,024 (0.7%)

Table 1: Number of 10-second speech recordings by language (total: 445,216) and corresponding percentage of the total dataset. Detailed statistics on the training and test datasets are provided in Supplementary Information (Tables Supp. 1 to Supp. 3). * = Language present in the Ramus corpus [Ramus et al., 1999].

2.3 Model architecture

A simplified diagram of the main version of the recurrent neural network implemented for the language identification task is shown in Fig. 2. The network inputs are vectors of dimension 6 regrouping the three normalized features presented in the previous subsection (values between 0 and 1) as well as the associated deltas (differences between two time steps). The network contains two hidden layers of 150 Long Short-term Memory (LSTM) units with forget gates [Gers et al., 2000]. The main benefit of LSTM networks over standard recurrent neural networks is to avoid the vanishing gradient problem during training [Hochreiter and Schmidhuber, 1997]. Each unit is associated with a hidden state but also a cell state which serves as a memory. The action of the output layer consists in linearly combining the hidden states of the second LSTM layer and applying the softmax operation. The result is an output vector \hat{y} that can be interpreted as a probability distribution indicating the likelihood of each language in the dataset being the language of the current input. Considering that the languages are indexed from 1 to 21 (1= German, 2=English, etc.), the desired output for a single recording is represented by a one-hot vector y that has only zeros except for the coordinate corresponding to the correct language; i.e.,

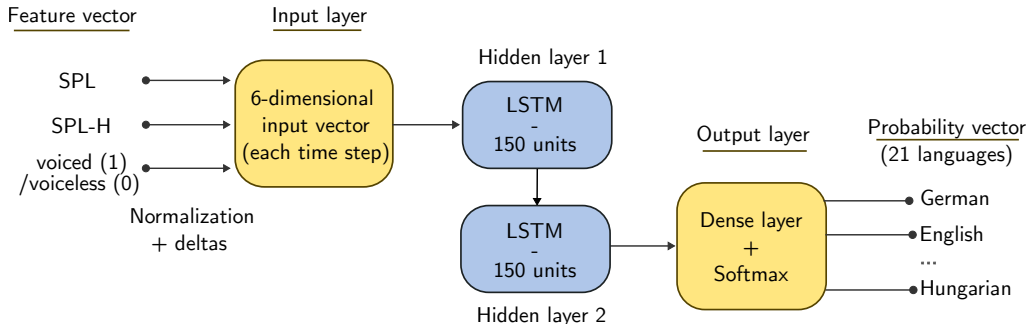


Figure 2: Block diagram of the recurrent neural network used for the language identification task. The input layer consists of the three features and the associated deltas (differences between two time steps) sampled at 31.25 Hz. The two hidden layers contain 150 LSTM units each; the model output after applying the softmax function can be interpreted as a probability vector of the most likely languages identified by the network.

of the form $\mathbf{y} = [0, \dots, 0, 1, 0, \dots, 0]$. The recurrent neural network is then trained to minimize the cross-entropy between the desired and generated vectors $H(\mathbf{y}, \hat{\mathbf{y}}) = -\sum_i y_i \log(\hat{y}_i)$, averaged over all time-steps.

The model was implemented using Keras and TensorFlow [Abadi et al., 2016]. It was optimized by batch gradient descent using the truncated backpropagation algorithm with truncated sequences of 32 time steps corresponding to about one second. The 10-second recordings were therefore divided into 10 slices to compute the gradients, but the LSTM states were reinitialized only at the presentation of a new recording. Nesterov’s accelerated gradient scheme was applied with a momentum of 0.9. The learning rate was initially set to 0.2 and was reduced to 93% of its value at each epoch. We used dropout [Srivastava et al., 2014] as a regularization method (recurrent dropout [Semeniuta et al., 2016]: 0.1, dropout between recurrent layers: 0.1, dropout for the dense layer: 0.2). A data augmentation scheme was used by applying a gentle distortion to the inputs: for each new batch, the identity mapping $[0,1]$ was replaced by the sum of six sigmoids evenly placed on the segment $[0,1]$ whose maximum slope varied from the unity by a random angle (standard deviation: $\pi/10$; contraction factor for the sigmoids: 15).

The dataset was split into a training and a test set (8% of the data) with different speakers to evaluate the performance of the model. The classification error and top-3 error were monitored during training using TensorBoard [Abadi et al., 2016]. The top-3 error is the proportion of recordings for which the three most likely languages identified by the network do not include the correct label. The classification error and top-3 errors were only based on the model output at the end of each 10-second recording, not the intermediate outputs. The model was trained on 25 epochs; i.e., each recording was used 25 times during training to update the model. This number of epochs corresponded to the point where the accuracy on the test set stopped improving (early stopping) to limit overfitting. Since the distribution of recordings across languages and speakers was not even for the training set, the overall contribution of each language and speaker was set to match saturating functions. More explicitly, for a given language, a variable n_{spk} was defined as $n_{spk} = \sum_s n(s)/(K1 + n(s))$ where $n(s)$ is the number of recordings for the speaker s . Then each sample associated with the speaker s was attributed the following weight in the loss function: $1/(K2 + n_{spk}) \cdot 1/(K1 + n(s))$, with $K1 = 20$, $K2 = 5$. The number of recordings by languages was more even for the test set (see Supplementary Figure Supp. 5).

It is important to note that performance was not the only criterion for selecting the architecture and the hyperparameters. In particular, we oriented the choice of the architecture towards smaller networks to force the model to learn shared representations across languages. Although larger networks may exhibit better performance, they tend to produce more independent clusters as shown by visualization methods such as t-SNE (see next subsection). This observation suggests that larger networks developed specialized parts for recognizing specific languages, i.e. they overfit the data, while rhythmic features should remain as general as possible. For the same reason, we combined different strategies of dropout to encourage the network to rely on a reduced number of activated units. Roughly, networks containing less than 100 units per layer had lower and more variable accuracy, whereas networks with over 200 units showed signs of overfitting to the languages of the dataset. We opted for 150 units per layer for the main version of the model as a trade-off between these two tendencies. Architectures with 3 hidden layers achieved similar performance as the 2-layer model, but were more difficult to train, therefore we only consider 2-layer models in the Results section.

2.4 Visualization methods

To inspect the model internal representation of languages after training, we carried out several visualization methods and clustering analyses based on the output probability vectors, using the following techniques:

- metric multidimensional scaling (MDS)
- hierarchical clustering
- t-distributed stochastic neighbor embedding (t-SNE) [van der Maaten and Hinton, 2008].

We used the implementations of scikit-learn for the three methods [Pedregosa et al., 2011]. The first two techniques require single high-dimensional vectors representing each class. For those, we used histograms of the last layer activations computed on a small balanced set of 6 720 recordings (320 recordings x 21 languages) sampled randomly from the larger dataset. More explicitly, let z_n be the output probability vector obtained at the end of the n -th recording; we define the vector ω_i representing the i -th language such as $[\omega_i]_n = \frac{[z_n]_i}{\sum_k [z_k]_i}$, where $[z_n]_i$ denotes the i -th component of the vector z_n . Several dissimilarity measures can be derived from the vectors ω . The results presented in the paper were obtained by applying the square root to each component of the vectors (normalization of the Euclidian norm) and by comparing them using the Euclidean distance (Hellinger distance) or minus the logarithm of their cross-product (Bhattacharyya distance). The pairwise comparisons were stored in a dissimilarity matrix that was then used as input for the MDS or hierarchical clustering methods. The Bhattacharyya distance quantifies the overlap between two probability distributions. For instance, if two normal distributions with the same variance are separated by 2 (or 4) standard deviations (measured by the gap between their means), the corresponding Bhattacharyya distance is 0.5 (or 2).

The t-SNE method differs from MDS as it seeks to faithfully render short- and medium-range proximities between points rather than to capture the general topology, which is fundamentally different for objects living in a high dimensional space. The t-SNE algorithm is based on a probabilistic interpretation of proximity by assuming a random sampling of point pairs for which nearby points are drawn with a higher probability. Two probability distributions are therefore defined, one in the initial space and the other in the low-dimensional embedding 2-d space. The algorithm aims to minimize a cross-entropy term between the two distributions. We refer the interested reader to Wattenberg et al. [2016] for more insights into the t-SNE method and its interpretation. For this analysis, 150 recordings by language were selected and the output probability vectors z_n (normalized through square root transformation) were used as the points to visualize. The t-SNE algorithm has a free parameter, the perplexity, which corresponds to the approximate number of neighbors of each point. The perplexity was set to the number of points by class (150).

It is worth noting that we chose to keep the dropout regularization to perform the analyses described above, even though the dropout of network units is usually removed post-training. This choice was motivated by the known fact that DNNs tend to show overconfidence in their predictions even though the classification accuracy does not warrant it. In the absence of dropout, the correlation between vectors representing different languages would typically be low, hindering the visualization methods. A mathematical interpretation of this strategy is presented in Gal and Ghahramani [2016].

2.5 Comparison with speech metrics

The analyses mentioned in the previous paragraphs do not reveal which features the network relies on to make its predictions. The resulting visualizations also lack interpretable axes. Previous work on rhythm metrics allowed for more direct explanations because the construction of the metrics was explicit, based on consonant-vowel segmentation. To fill the interpretative gap between the two approaches, we tested whether the features learned by the recurrent neural network were correlated with known rhythm metrics. To this end, we used the Ramus corpus [Ramus et al., 1999], in which sentences were already segmented into consonants (C) and vowels (V). The rhythm metrics considered were the following:

- %V: the proportion of time covered by the vocalic intervals, ΔC : the standard deviation of consonantal intervals, ΔV : the standard deviation of vocalic intervals [Ramus et al., 1999]
- Varcos: the same metrics as above but ΔC (resp. ΔV) is divided by the mean consonantal (resp. vocalic) interval duration [Dellwo, 2006]
- the *pairwise variability indexes* (PVIs) [Grabe and Low, 2002]

Raw PVIs and normalized PVIs are defined by the following equations:

$$rPVI = \sum_{k=1}^{m-1} |d_{k+1} - d_k| / (m - 1)$$

$$nPVI = \sum_{k=1}^{m-1} \left| \frac{d_{k+1} - d_k}{(d_{k+1} + d_k)/2} \right| / (m - 1),$$

where d_k denotes the duration of the k -th consonantal or vocalic interval. Consistent with the rest of the literature, we considered raw PVIs for consonantal intervals ($rPVI_C$) and normalized PVIs for vocalic intervals ($nPVI_V$).

The different metrics were computed for each sentence of the Ramus corpus for which the segmentation was available (160 sentences from the following 8 languages: French, English, Dutch, Polish, Spanish, Italian, Catalan, Japanese). The same sentences were provided as inputs to the neural network and the activations of the first and second hidden layers at the end of the sentences were stored.

We employed two strategies to examine the correlations between the rhythm metrics and the model activations. The first strategy was to test if the correlation between single cell activations and the rhythm metrics was significant using the Pearson coefficient (r) and the Bonferroni correction for multiple testing, assuming the normality of both activation and metric values. The second strategy consisted in mapping the rhythm metrics to linear combinations of cell activations within a hidden layer. For this analysis, we used a linear regression model with a regularized least squares method due to limited available data. More specifically, we adopted the ElasticNet [Zou and Hastie, 2005] implementation of scikit-learn [Pedregosa et al., 2011]. The ElasticNet’s objective function is of the form $1/(2n)\|y - Xw\|_2^2 + \alpha r_1 \|w\|_1 + \alpha(1 - r_1)\|w\|_2^2/2$. r_1 was set to 0.2 and α was determined through a cross-validation procedure with 7 folds. The metrics were normalized beforehand to ensure that the vectors y had a quadratic norm of 1. The results of the regression analysis were then used to generate language maps embedded in 2-d feature spaces.

3 Results

3.1 Language discrimination

The trained model with 2×150 units was able to recognize the language of the 10-second recordings 41% of the time on the test set (on training set: 50%), and the correct language was in the top 3 guesses of the network 67% of the time (on training set: 80%). Figure 3a and 3b shows the evolution of accuracy during training; Fig. 3c shows the average accuracy at different time points within the recordings. Although the training and test datasets have different speakers, they originate from the same databases and share correlated characteristics. The presented results are therefore likely higher than the actual performance measured on a independent speech dataset. Indeed, the accuracy on 3-second recordings of the Ramus corpus is 18% (top 3 accuracy: 42%), compared to 25% at 3 seconds on our dataset (Fig. 3c).

A larger network of 2×180 units and no dropout for the last layer achieved an accuracy of 57% on the test set, and a top-3 accuracy of 79%. With the addition of F0, the same model reached 61% in accuracy and 82% for top-3 accuracy. We show the results obtained with this higher-performing model in Supplementary Information (Fig. Supp. 11 to Supp. 15). The main difference is that the individual languages are more distant from each other in the activation-based representational spaces, indicating a higher level of specialized processing for each language. The results, however, align with those of the small model that the rest of the results presented below are based on.

The confusion matrix restricted to the eight languages of the Ramus corpus is displayed in Fig. 4; the full matrix can be found as Supplementary Fig. Supp. 6. The confusion matrix alone does not reveal any clear cluster or groups of languages. To further investigate if such groups can be extracted from model confusion patterns, we carried out proximity analyses on histograms computed from the activations of the output layer. Fig. 5a shows a dendrogram built from a hierarchical clustering method with complete linkage using the Bhattacharyya distance. The y-axis corresponds to the maximum distance between languages of two clusters when they are merged to form a larger group. The dendrogram displayed represents only one possible version: the specific arrangement of languages can vary depending on the distance or the linkage method used, as well as the version of the neural network considered for analysis. This is especially true for the languages that are well discriminated by the neural network, corresponding to the languages with a high junction point on the diagram (including Asian languages). To illustrate this point, we show other versions of the dendrogram generated for the same DNN using an information-theoretic distance or a different linkage method in Supplementary Fig. Supp. 7. The right part of the dendrogram illustrated in Fig. 5a, on the contrary, was found to be more robust to changes in method parameters. The first paired languages are Dutch and German, followed by Italian and Spanish (Bhattacharyya distances: 0.71 and 0.76). The next pairs of languages are French and Turkish, then Portuguese and Russian (distances: 0.91 and 1.14).

The representation of languages based on the network activations can be further investigated using the MDS and t-SNE visualization tools (Fig. 5b and Fig. 6). The two figures provide similar results and clarify the relative positioning of the language groups previously mentioned. In particular, French, Turkish, Russian and Portuguese, are found to occupy an

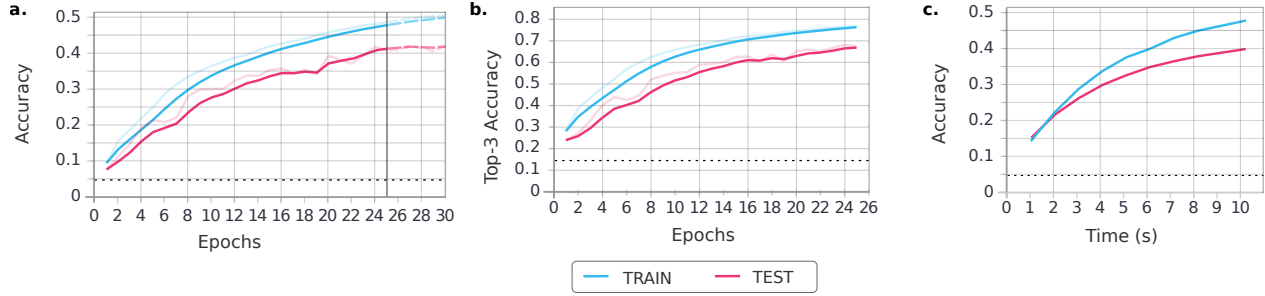


Figure 3: **(a)** Model accuracy and **(b)** top-3 accuracy during training as a function of epoch for the language identification task. After 25 epochs corresponding to the trained version presented in the paper (early stopping), the test accuracy stopped improving. **(c)** Mean accuracy after training at different time points within the recordings (0= start of recordings, 10 sec=end of recordings). The horizontal dashed lines indicate the chance levels assuming equiprobability of the language classes. Light lines: raw numbers; dark lines: smoothed data; colored dashed lines: data between epochs 26 and 30 (for reference).

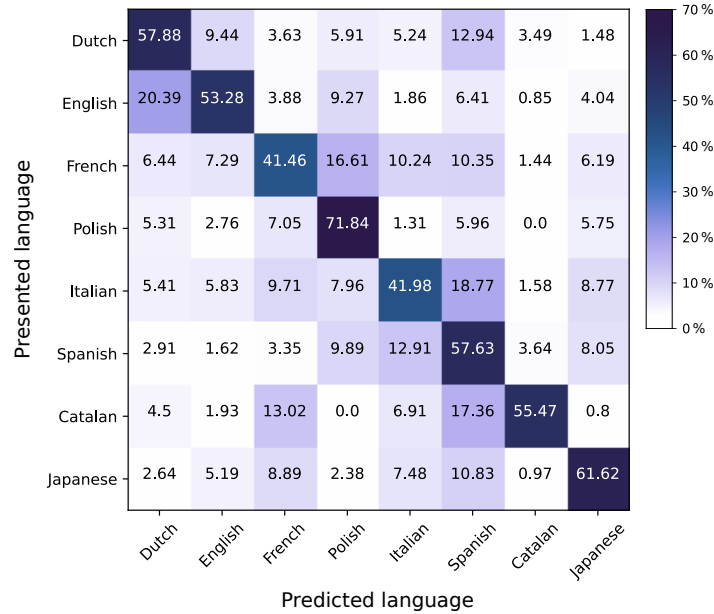


Figure 4: Confusion matrix on the test set for a limited number of languages (languages from the Ramus corpus [Ramus et al., 1999]). The figures correspond to percentages (normalized by row). The entire confusion matrix is provided as Supplementary Fig. Supp. 6.

intermediate position between the stress-timed Germanic languages (English, German, Dutch), and the cluster dominated by syllable-timed languages (including Spanish and Italian). The MDS analysis in Fig. 5b only included the languages corresponding to the right part of the dendrogram to achieve a stress (MDS cost function) below 0.2. By contrast, the t-SNE plot (Fig. 6), which focuses on preserving local proximity rather than the global topology, includes all the languages of the dataset. However, similar to the left part of the dendrogram, interpreting the results should be approached with caution for the languages that are well discriminated by the network, forming independent clusters in the t-SNE plot. Their relative positioning is more sensitive to the samples provided as input or the algorithm’s initialization compared to the denser central cluster.

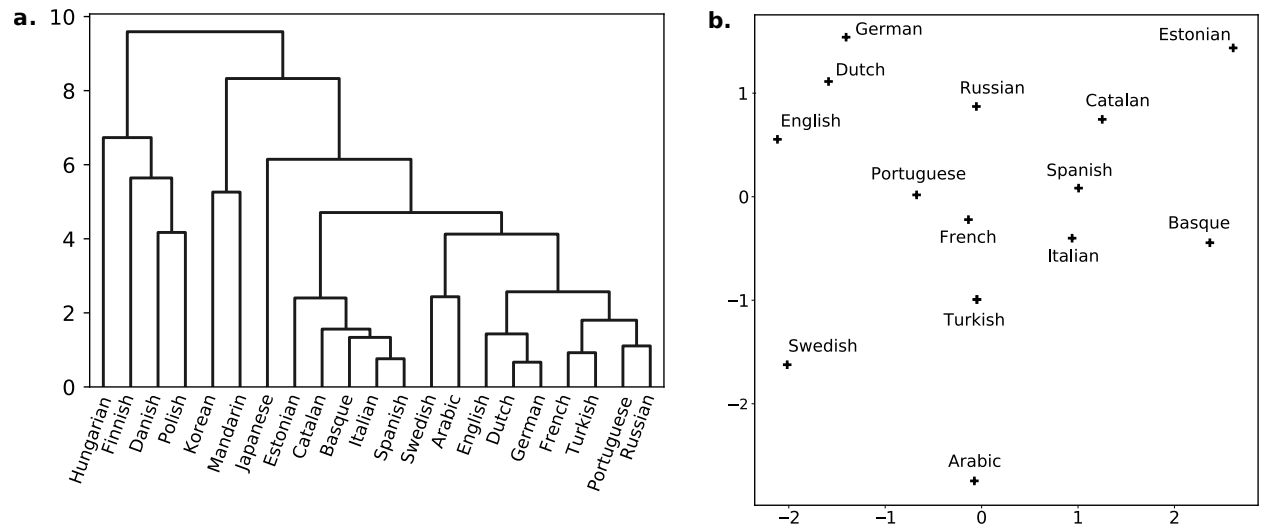


Figure 5: **(a)** Hierarchical clustering dendrogram based on histograms of the DNN probability vector output using the complete linkage method and the Bhattacharyya distance. **(b)** Metric dimensional scaling (MDS) visualization for the languages in the right branch of the dendrogram, also based on the Bhattacharyya distance between activation histograms. MDS stress: 0.14.

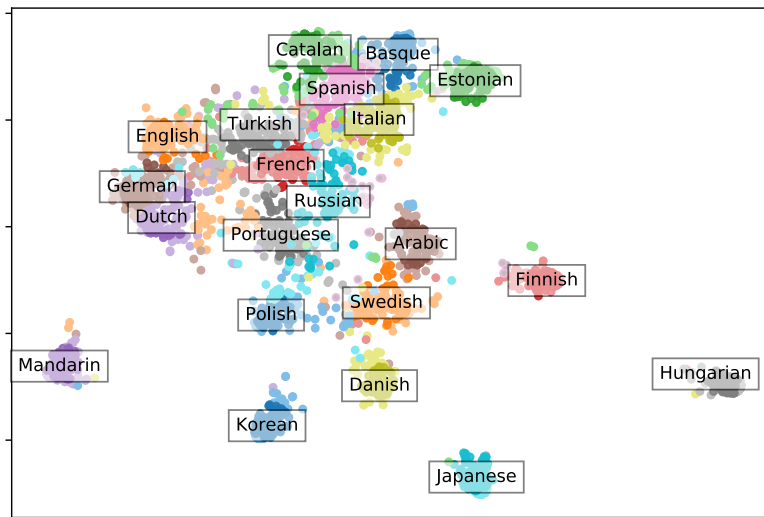


Figure 6: One output of the t-SNE algorithm based on the output probability vectors of single samples, represented by each point, and the Hellinger distance. Labels and colors correspond to the predicted language, i.e. the language as seen by the model. Number of samples by classes and perplexity: 150.

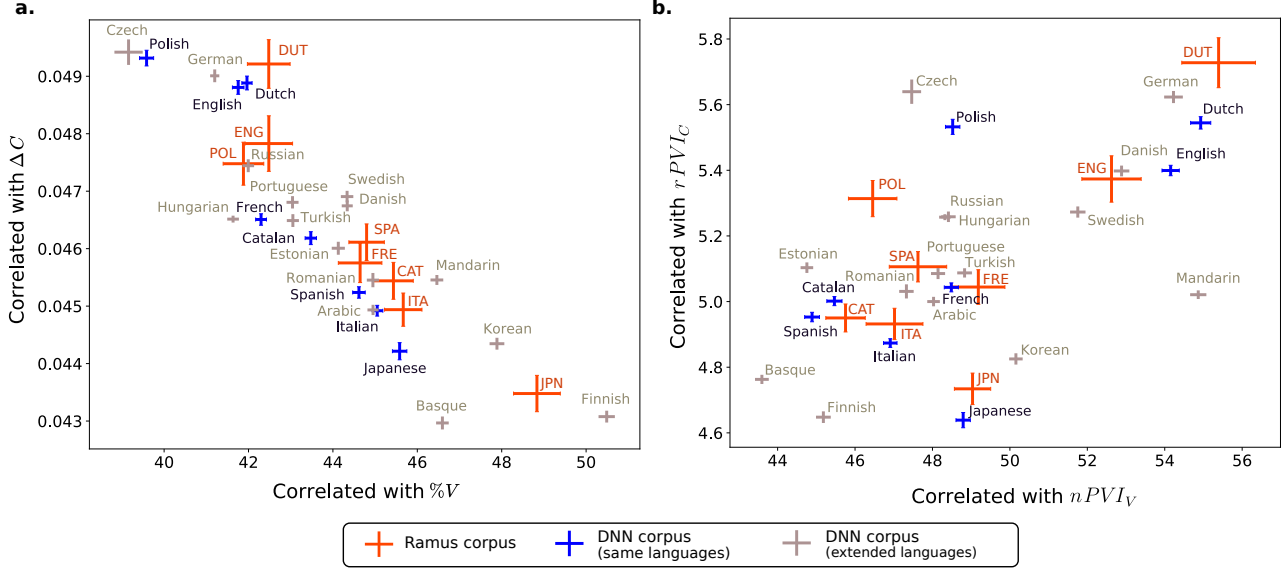


Figure 7: Language maps in spaces defined by linear combinations of learned features (hidden layer activations) correlated with rhythm metrics (based on the Ramus corpus and ElasticNet). The axes are defined by the correlates of (a) ($\%V$, ΔC) and of (b) ($nPVI_V$, $rPVI_C$). The error bars correspond to standard error, for data averaged over the Ramus corpus (red crosses, short form labels) and over 7,000 recordings from our dataset (blue and grey crosses).

3.2 Correlations with rhythm metrics

To enhance the interpretability of our model, we tested whether some of the learned features, encapsulated by the hidden layer activations, were correlated with established rhythm metrics. On the Ramus corpus [Ramus et al., 1999], we found that the rhythm metric presenting the highest correlation with a single cell activation was $\%V$ ($r=0.52$, $p<1e-4$ assuming independent Gaussian variables with Bonferroni correction), followed by $nPVI_V$ ($r=0.47$, $p<1e-4$), the PVI index for vocalic intervals. The fact that the highest correlation was found for $\%V$ (proportion of duration covered by vocalic intervals) was not surprising as it is a relatively simple feature to learn. The other metrics in the order of decreasing Pearson coefficient were: ΔC ($r=0.45$, $p<1e-4$), $rPVI_C$ ($r=0.40$, $p<1e-4$), ΔV ($r=0.37$, $p<1e-3$), and the Varcos ($r=0.3$, $p=0.05$). Most high correlations between rhythm metrics and cell activations were found within the second hidden layer. Supplementary Information provides two language maps based on these single cell activations (Supplementary Fig. Supp. 8 and Supp. 9).

Because the information corresponding to rhythm metrics may be distributed across several cells, we also considered linear combinations of neural units using the results of linear regressions between the activations of the second hidden layer and the rhythm metrics. We used this analysis to generate plots analogous to maps based on rhythm metrics. The maps for the correlates of ($\%V$, ΔC) and ($nPVI_V$, $rPVI_C$) are shown in Fig. 7. The figure for the correlates of (ΔV , ΔC) is similar to the figure for the PVI; it can be found as Supplementary Fig. Supp. 10 online. The red crosses represent the combination of activations computed on the Ramus corpus. Since these recordings were used to find the correlates, the red crosses are naturally arranged in a similar manner to the maps based on rhythm metrics using the same corpus [Ramus, 2002]. The blue crosses represent the same languages but with scores computed on a larger corpus (320 recordings by languages from our dataset). The overall proximity of red and blue crosses for the same languages gives us confidence that the regression model was still valid beyond the initial dataset. This can be quantified by comparing the variance between languages to the variance within each language, which also gives an indication of the variability of the captured features. In decreasing order of the variance ratio, we find the correlates of $rPVI_C$ ($F(7,8)=26$, $p<1e-4$), $nPVI_V$ ($F(7,8)=25$, $p<1e-4$), ΔC ($F(7,8)=16$, $p<1e-3$), and $\%V$ ($F(7,8)=5.2$, $p=0.02$). After this step, all the other languages of the DNN model were included to provide a map with the 21 languages (gray crosses). We also added Czech and Romanian that were not used for the training of the DNN due to insufficient data – note that Czech was most often classified as Polish (55% of the times) by the DNN and Romanian as Russian (25% of the times).

A natural question that can arise from the analyses with the correlated features is how much information used by the neural network for the discrimination task is available in these feature spaces. To address this question, we conducted a quadratic discriminant analysis (QDA) in the space composed by the correlates of the four metrics ($\%V$, ΔC , $nPVI_V$, $rPVI_C$).

The QDA classifier achieved an accuracy of 36% on the training set (top-3: 60%) and 25% on the test set (top-3: 47.5%). These scores represent 60% to 80% of the performance achieved by the DNN. We also tested the QDA model restricted to the five languages included in Loukina et al. [Loukina et al., 2011] (except for Greek replaced by Spanish). We found an accuracy of 50% on the test set, comparable to the average score of 46% reported by the authors for classifiers using four rhythm metrics on recordings of entire paragraph readings. On the test set with the same restriction of languages, the neural network achieved 62% accuracy.

4 Discussion

We developed a recurrent neural network to identify languages on the basis of rhythmic features. We could investigate how languages were related or separated by the network using clustering and visualization techniques based on the network output probability vectors. A third of the languages, corresponding to the left branch of the dendrogram in Fig. 5, were individually well separated, and their arrangement relative to the other languages was variable. The clustering of the other part of the languages could be interpreted more consistently. The Germanic stress-timed languages (English, Dutch, German) were systematically grouped together, as were Spanish and Italian (prototypical syllable-timed languages). Considering larger clusters on the dendrogram, the results were overall consistent with the traditional dichotomy of languages, but presented some fine-grained differences. Spanish and Italian were grouped together with Basque, Catalan and Estonian, while the latter two languages have sometimes been described as having a mixed rhythm [Grabe and Low, 2002]. The Germanic languages formed a larger group with other stress-timed languages (e.g., Portuguese, Russian), but this group also contained Turkish and French, generally considered as syllable-timed. The MDS or t-SNE visualizations however positioned French and Turkish, in addition to Portuguese and Russian, between the groups of stress- and syllable-timed languages.

The regression analysis between the hidden states of the recurrent neural network and rhythm metrics, first conducted on the languages of the Ramus corpus [Ramus et al., 1999] and extended to the 21 languages of our dataset, revealed that several dimensions of the DNN inner representation encodes features highly correlated with rhythm metrics, allowing interpretations in line with previous work. Figure 7 shows the placement of the languages on feature maps whose axes are correlated with these metrics. The correlates of ($\%V$, ΔC) (Fig. 7a) exhibit a stress-timed to syllable-timed gradient, with stress-timed languages associated with a lower value for the correlate of $\%V$, the percentage of time covered by vocalic intervals, and a higher value for the correlate of ΔC , supposedly reflecting syllable structure complexity. Most of the points within the plot are found on the same diagonal, consistent with the previous observation that $\%V$ and ΔC are highly correlated [Ramus, 2002], making it difficult to distinguish the properties represented by the two axes. Despite the apparent gradient of stress- and syllable-timing, it cannot be concluded that all languages are distributed according to this rule based on the traditional categorization of languages. For example, Czech appears at the upper left corner of the plot, but is sometimes classified as syllable-timed. The positioning of Czech in the plots of Fig. 7 is however consistent with a previous study which found that Czech is within the cluster of stress-timed languages for $\%V$ and $rPVI_C$, but not for $nPVI_V$ [Dellwo, 2007]. Conversely, Arabic is generally considered to be stress-timed but is found in the lower right quadrant in panel A. The points computed on the Ramus corpus (red crosses) exhibit the three separated classes that were described by the authors of the original study (syllable-, stress- and mora-timed languages [Ramus, 2002]), but this separation in three classes does not generalize to our dataset including more languages. The distribution of points is rather in line with the idea of a continuum advocated by Dauer, among others, [Dauer, 1983, Nespore, 1990] and supported by other studies based on rhythm metrics [Grabe and Low, 2002, Mairano, 2011]. Note that, if we were to adhere to the separation in three classes suggested in Ramus et al., Finnish, Basque and Korean would be categorized as presenting mora-timed features. The figure with the correlates of the PVIs (Fig. 7b) exhibits a similar gradient with syllable-time languages occupying the left lower part of the figure and stress-timed languages occupying the right upper part. This configuration is assumed to reflect the fact that stress-timed languages are marked by greater variability in vocalic and inter-vocalic interval lengths. However, for this second figure, a few languages depart from the main diagonal. This is the case especially for Czech and Polish, which occupy the upper left quadrant of the plot. This result aligns with previous studies using rhythm metrics [Ramus, 2002, Grabe and Low, 2002, Dellwo, 2007] and is consistent with the observation that these two languages are characterized by complex consonantal clusters but no vowel reduction at normal speech rates.

While we have provided evidence that DNNs are useful tools to detect rhythmic features of languages, our work has certain limitations. We have used a strongly degraded signal, leaving only the amplitude envelope and voicing information, in order to restrict the input to prosodic features. We know, however, that even a severely degraded speech signal consisting of only a few amplitude envelopes can provide enough phonetic information for adults to comprehend speech under ideal listening conditions, i.e., in silence [Shannon et al., 1995]. This has motivated our choice to use medium-sized neural networks instead of larger networks that would integrate more phonetic or linguistic knowledge. But, even without a fine-grained processing of phonetic features, the DNN could still capture broad phonological regularities. For example, Portuguese and Russian could be close in the representational space, not only because of prosody, but because of other similarities, such as

the extensive use of sibilant fricatives, easily recognized as weak segments with spectral energy mainly contained in the medium or high frequencies. In that regard, the correlation analysis with rhythm metrics helped to disentangle contributing factors and provide more interpretation to the visualisations derived from the network activations. This does not completely resolve the issue – in fact, even rhythm metrics have been criticized by a few authors for relying too much on phonological factors without a direct link to prosody [Kohler, 2009b, Arvaniti, 2009]. As we also argue in the next paragraphs, these valid points should not hold too strict standards for exploratory work in speech rhythm. Since the works of Dauer [Dauer, 1983] and Bertinetto [Bertinetto, 1989] who promoted the view that phonology and rhythm are not independent but intertwined dimensions of speech production and perception, the search for phonological or acoustic correlates of linguistic rhythm has been productive in finding measurable bases for the intuitive notion of rhythmic classes among languages. The present study fully embraces this line of research by relying on a statistical language-identification model with only acoustic features as its input. It is important to note that while this approach has several merits (e.g., avoiding reliance on a priori segmental division of speech, incorporating aspects of phone quality or co-articulation), models that incorporate more abstract elements of phonological segmentation may be equally valid to investigate speech rhythm. As an example, a DNN model based on the durations of phonetic segments and CV clusters was developed to identify the prosody of native vs non-native English speakers [Kyriakopoulos et al., 2019]. The extension and analysis of such models could provide complementary and valuable information about the statistical regularities related to speech rhythm.

Our approach exploits the remarkable effectiveness of recurrent neural networks for pattern-recognition tasks when a large number of labeled examples is available for training [Beaufays et al., 2014, Karpathy et al., 2016]. Among the multiple strengths of DNNs, they are efficient in handling factors of intra-class variability, such as changes in speech rate, a known common issue for rhythm metrics [Ramus, 2002, Arvaniti, 2009, Mairano, 2011]. By relying on a DNN instead of explicit phonological metrics, we could bypass the costly task of manually annotating consonant-vowel segments. That way, more languages could be included in the feature maps. But the value of DNNs extends well beyond these practical advantages. DNNs have the capacity to learn and generalize multiple complex patterns from statistical regularities found in the training data, achieving a greater degree of expressivity than metrics, which by contrast are aggregate measures coding for a coarse aspect of timing [Arvaniti, 2009, Turk and Shattuck-Hufnagel, 2013]. This allows our model to reach good accuracy at the level of a few sentences, while classifiers based on rhythm metrics typically work on larger sets or considering a reduced number of rhythmically distinct languages [Ramus et al., 1999, Arvaniti, 2009]. We showed that a QDA classifier trained on the 4th-dimensional DNN feature subspace correlated with speech metrics (Fig. 7) matched the performance of comparable classifiers using rhythm metrics [Loukina et al., 2011], but on recordings of shorter durations. These low-dimensional classifiers were outperformed by the full DNN model (62% accuracy vs 50% accuracy considering five languages).

DNNs shift modeling from low-dimensional analytical approaches to statistical models that have superior predictive power but are also more opaque – a criticism of DNNs being that they do not offer a straightforward interpretation of how they map inputs and outputs (commonly referred to as the ‘black-box’ problem). For this reason, the use of DNNs in cognitive science represents a major paradigm shift for the modeling of perception or sensory systems [Kell and McDermott, 2019, Cichy and Kaiser, 2019, Storrs and Kriegeskorte, 2019]. In this last paragraph, we mention several important aspects of this methodological evolution that provide further context for our approach. First, although the lack of interpretability is a legitimate criticism of DNNs, they are also well suited for post-hoc analyses that mitigate this issue [Cichy and Kaiser, 2019, Storrs and Kriegeskorte, 2019]. The linear mapping of features with rhythm metrics in this study is one example, but some DNNs can be analyzed in much greater detail, as it has been done in visual object recognition [Cammarata et al., 2020]. Much information about DNN behavior can be gained from running the model on custom-made stimuli: in our case, these could be stereotypical rhythmic patterns or resynthesized speech stimuli [Ramus and Mehler, 1999]. This type of approach has been fruitful for investigating the sensitivity of DNNs to shape and how it compares to visual perception [Kubilius et al., 2016]. A second point is that some caution is required when interpreting the results of DNN models, especially when considering them as possible models of perception. Although a coarse measure of model performance can be reminiscent of error patterns found in perception studies (e.g., the discrimination abilities of young infants in our case [Ramus et al., 1999]), DNNs present biases that human subjects do not have. This is now well-documented, again in the area of visual perception [Wichmann and Geirhos, 2023]. Another cautionary note that certainly applies to our study is that appealing visualizations generated during DNN analyses are not sufficient for building scientific knowledge [Leavitt and Morcos, 2020]. They can give a sense of intuitive knowledge about the DNN behavior but they lack the rigor of more formal approaches. This view has to be nuanced by recognizing that the analysis of DNN behavior provides rich information about the statistical structure of complex stimuli that can lead to new developments and hypotheses on related cognitive concepts [Kell and McDermott, 2019]. Cichy and Kaiser reinforced this point by arguing that, although the drawbacks of DNNs complicate their use as explanatory models, they are invaluable tools for exploring cognitive theories that are not yet fully established [Cichy and Kaiser, 2019].

We think that Cichy and Kaiser’s argument is particularly relevant to speech rhythm research: despite a long history of developments, the field is still in an exploratory phase, due to the complexity of the underlying phenomena and the lack of a powerful tool to connect the intuition of linguists with concrete statistical regularities in the speech signal. Research on

speech rhythm is at a stage where it would certainly benefit from creative and diverse approaches using DNN models, that will have to be followed by more formal verifications of hypotheses and efforts to converge to a much needed [Turk and Shattuck-Hufnagel, 2013] unified view of speech rhythm. As in other areas of cognitive science, these advances would be facilitated by setting up interdisciplinary projects that bring together machine-learning experts and psychologists (and/or linguists), and by fostering the sharing of resources and models across labs [Storrs and Kriegeskorte, 2019].

Code and data availability

The code for training and running the model is available on <https://zenodo.org/doi/10.5281/zenodo.10211058>. We also provide the model weights for the main version discussed in the paper, as well as the regression coefficients for the comparison with speech metrics.

The training data was retrieved from publicly available datasets (<https://commonvoice.mozilla.org/en/datasets>, <https://github.com/larsyencken/wide-language-index>, <https://www.voxforge.org/>, <https://librivox.org/>, <https://tatoeba.org/>). The data from Ramus et al. 1999 was obtained from the authors of that study upon request. The parameters for the main version of the model discussed in the paper and the linear regression coefficients for the comparison with speech metrics are provided with the code.

Acknowledgements

We wish to thank Jean-Pierre Nadal for his valuable support as a member of the “SpeechCode” project and as F.D.’s supervisor during his PhD. We gratefully acknowledge the support of Violette Daures in carrying out a part of the analyses on the Ramus corpus. We also thank Christian Lorenzi and Ramon Guevara, two other members of the “SpeechCode” project, for their insightful input. Thanks to Franck Ramus for providing us with the speech samples and labeled data. This work was partly funded by the project “SpeechCode” of the French National Research Agency, the ANR, contract ANR-15-CE37-0009-03 (<http://www.agence-nationale-recherche.fr>), as well as the ECOS- Sud action nr. C20S02, the ERC Consolidator Grant 773202 “BabyRhythm”, the ANR’s French Investissements d’Avenir – Labex EFL Program under Grant [ANR-10-LABX-0083], the Italian Ministry for Universities and Research FARE grant nr. R204MPRHKE, the European Union Next Generation EU NRRP M6C2 - Investment 2.1 - SYNPHONIA Project, as well as the Italian Ministry for Universities and Research PRIN grant nr. 2022WX3FM5 to JG. A part of this work was conducted while F.D. was on a postdoctoral fellowship supported by Fondation Pour l’Audition (FPA RD-2019-3).

References

- T Nazzi, J Bertoncini, and Jacques Mehler. Language discrimination by newborns: Toward an understanding of the role of rhythm. *Journal of experimental psychology. Human perception and performance*, 24(3):756–66, June 1998.
- Jacques Mehler, Anne Christophe, and Franck Ramus. What we know about the initial state for language. *Image, Language, Brain: Papers from the First Mind-Brain Articulation Project Symposium*, (33 1):51–75, 2000.
- Anne Cutler. Segmentation problems, rhythmic solutions. *Lingua*, 92:81–104, April 1994. ISSN 0024-3841. doi:10.1016/0024-3841(94)90338-7.
- Kenneth L. Pike. *The Intonation of American English*. University of Michigan (Ann Arbor), July 1945. doi:10.2307/409880.
- D Abercrombie. *Elements of General Phonetics*. University of Edinburgh, 1967.
- Peter Roach. On the distinction between ‘stress-timed’ and ‘syllable-timed’ languages. *Linguistics Controversies*, pages 73–79, 1982.
- Rebecca M. Dauer. Stress-timing and syllable-timing reanalyzed. *Journal of Phonetics*, 11:51–62, 1983.
- Alan Langus, Jacques Mehler, and Marina Nespor. Rhythm in language acquisition. *Neuroscience & Biobehavioral Reviews*, 81:158–166, October 2017. ISSN 0149-7634. doi:10.1016/j.neubiorev.2016.12.012.
- Jacques Terken and Dik Hermes. The Perception of Prosodic Prominence. In *Prosody: Theory and Experiment*, pages 89–127. 2000. doi:10.1007/978-94-015-9413-4_5.
- Pier Bertinetto. Reflections on the dichotomy ‘stress’ vs. ‘syllable-timing’. *Revue de phonétique appliquée*, 91(93):99–130, 1989.
- Klaus J Kohler. Rhythm in Speech and Language. *Phonetica*, 66(1-2):29–45, 2009a. ISSN 0031-8388. doi:10.1159/000208929.
- Ruth Elizabeth Cumming and F. Nolan. *Speech Rhythm: The Language-Specific Integration of Pitch and Duration*. PhD thesis, 2010.

- Alice Turk and Stefanie Shattuck-Hufnagel. What is speech rhythm? A commentary on Arvaniti and Rodriguez, Krivokapić, and Goswami and Leong. *Laboratory Phonology*, 4(1):93–118, 2013. ISSN 1868-6346. doi:10.1515/lp-2013-0005.
- Franck Ramus, Marina Nespoulet, and Jacques Mehler. Correlates of linguistic rhythm in the speech signal. *Cognition*, 73(3): 265–292, 1999. ISSN 00100277. doi:10.1016/S0010-0277(99)00058-X.
- Esther Grabe and Ee Ling Low. Durational variability in speech and the Rhythm Class Hypothesis. In *Laboratory Phonology 7*, pages 515–546. 2002. ISBN 978-3-11-019710-5. doi:10.1515/9783110197105.
- Christine Moon, Robin Panneton Cooper, and William P. Fifer. Two-day-olds prefer their native language. *Infant Behavior and Development*, 16(4):495–500, October 1993. ISSN 0163-6383. doi:10.1016/0163-6383(93)80007-U.
- Judit Gervain and Jacques Mehler. Speech perception and language acquisition in the first year of life. *Annual review of psychology*, 61:191–218, 2010.
- Konstantinos Kyriakopoulos, Kate M. Knill, and Mark J.F. Gales. A Deep Learning Approach to Automatic Characterisation of Rhythm in Non-Native English Speech. In *Interspeech 2019*, pages 1836–1840. ISCA, September 2019. doi:10.21437/Interspeech.2019-3186.
- Amalia Arvaniti. Rhythm, Timing and the Timing of Rhythm. *Phonetica*, 66:46–63, 2009. doi:10.1159/000208930.
- Lukas Wiget, Laurence White, Barbara Schuppler, Isabelle Grenon, Olesya Rauch, and Sven L. Mattys. How stable are acoustic metrics of contrastive speech rhythm? *The Journal of the Acoustical Society of America*, 127(3):1559–1569, March 2010. ISSN 0001-4966. doi:10.1121/1.3293004.
- Amalia Arvaniti. The usefulness of metrics in the quantification of speech rhythm. *Journal of Phonetics*, 40(3):351–373, May 2012. ISSN 00954470. doi:10.1016/j.wocn.2012.02.003.
- Tamara V. Rathcke and Rachel H. Smith. Speech timing and linguistic rhythm: On the acoustic bases of rhythm typologies. *The Journal of the Acoustical Society of America*, 137(5):2834–2845, May 2015. ISSN 0001-4966. doi:10.1121/1.4919322.
- Daniel L K Yamins and James J DiCarlo. Using goal-driven deep learning models to understand sensory cortex. *Nature Neuroscience* 2016 19:3, 19(3):356–365, February 2016. ISSN 1546-1726. doi:10.1038/nn.4244.
- Alexander Je Kell and Josh H McDermott. Deep neural network models of sensory systems: Windows onto the role of task constraints. *Current Opinion in Neurobiology*, 55:121–132, 2019. doi:10.1016/j.conb.2019.02.003.
- Katherine R Storrs and Nikolaus Kriegeskorte. Deep Learning for Cognitive Neuroscience. In M Gazzaniga, editor, *The Cognitive Neurosciences, 6th Edition*. MIT Press, 2019. ISBN 1903.01458v1.
- Yann LeCun, Yoshua Bengio, and Geoffrey Hinton. Deep learning. *Nature*, 521(7553):436–444, May 2015. ISSN 0028-0836, 1476-4687. doi:10.1038/nature14539.
- Alex Krizhevsky, Ilya Sutskever, and Geoffrey E Hinton. ImageNet classification with deep convolutional neural networks. *Communications of the ACM*, 60(6):84–90, 2017. ISSN 15577317. doi:10.1145/3065386.
- Dong Yu and Li Deng. *Automatic Speech Recognition : A Deep Learning Approach*. Springer London, London, 2015. doi:10.1007/978-1-4471-5779-3.
- Sepp Hochreiter and Jürgen Schmidhuber. Long Short-Term Memory. *Neural Computation*, 9(8):1735–1780, November 1997. ISSN 0899-7667. doi:10.1162/neco.1997.9.8.1735.
- Rosana Ardila, Megan Branson, Kelly Davis, Michael Henretty, Michael Kohler, Josh Meyer, Reuben Morais, Lindsay Saunders, Francis M Tyers, and Gregor Weber. Common voice: A massively-multilingual speech corpus. In *LREC 2020 - 12th International Conference on Language Resources and Evaluation, Conference Proceedings*, pages 4218–4222, 2020. ISBN 979-10-95546-34-4.
- Hedvig Skirgård, Sean G Roberts, and Lars Yencken. Why are some languages confused for others? Investigating data from the great language game. *PLoS ONE*, 12(4), 2017. ISSN 19326203. doi:10.1371/journal.pone.0165934.
- Gunnar Fant, Anita Kruckenberg, and Johan Liljencrants. Acoustic-phonetic Analysis of Prominence in Swedish. In *Intonation*, pages 55–86. Springer, Dordrecht, 2000. doi:10.1007/978-94-011-4317-2_3.
- Agaath M C Sluijter and Vincent J Van Heuven. Spectral balance as an acoustic correlate of linguistic stress. Technical report, 1996.
- Yannick Jadoul, Bill Thompson, and Bart de Boer. Introducing Parselmouth: A Python interface to Praat. *Journal of Phonetics*, 71:1–15, November 2018. ISSN 00954470. doi:10.1016/j.wocn.2018.07.001.
- Paul Boersma and David Weenink. Praat: Doing phonetics by computer, 2018.
- Felix Gers, Jürgen Schmidhuber, and Fred Cummins. Learning to Forget: Continual Prediction with LSTM. *Neural computation*, 12:2451–71, October 2000. doi:10.1162/089976600300015015.

- Martín Abadi, Paul Barham, Jianmin Chen, Zhifeng Chen, Andy Davis, Jeffrey Dean, Matthieu Devin, Sanjay Ghemawat, Geoffrey Irving, Michael Isard, et al. TensorFlow: Large-Scale Machine Learning on Heterogeneous Distributed Systems, March 2016.
- Nitish Srivastava, Geoffrey Hinton, Alex Krizhevsky, Ilya Sutskever, and Ruslan Salakhutdinov. Dropout: A Simple Way to Prevent Neural Networks from Overfitting. *Journal of Machine Learning Research*, 15(56):1929–1958, 2014. ISSN 1533-7928.
- Stanislau Semeniuta, Aliaksei Severyn, and Erhardt Barth. Recurrent dropout without memory loss. In *COLING 2016 - 26th International Conference on Computational Linguistics, Proceedings of COLING 2016: Technical Papers*, pages 1757–1766, 2016. ISBN 978-4-87974-702-0. doi:10.5281/zenodo.546212.
- Laurens van der Maaten and Geoffrey Hinton. Visualizing Data using t-SNE. *Journal of Machine Learning Research*, 1: 1–48, 2008.
- F Pedregosa, G Varoquaux, A Gramfort, V Michel, B Thirion, O Grisel, M Blondel, P Prettenhofer, R Weiss, V Dubourg, J Vanderplas, A Passos, D Cournapeau, M Brucher, M Perrot, and E Duchesnay. Scikit-learn: Machine Learning in Python. *Journal of Machine Learning Research*, 12:2825–2830, 2011.
- Martin Wattenberg, Fernanda Viégas, and Ian Johnson. How to Use t-SNE Effectively. *Distill*, 1(10):e2, October 2016. ISSN 2476-0757. doi:10.23915/distill.00002.
- Yarin Gal and Zoubin Ghahramani. Dropout as a Bayesian Approximation. In *33rd International Conference on Machine Learning, ICML 2016*, volume 3, pages 1661–1680, 2016. ISBN 978-1-5108-2900-8.
- V Dellwo. Rhythm and Speech Rate: A Variation Coefficient for deltaC. In *Language and Language-Processing*, number 1999, pages 231–241. 2006. ISBN 3-631-50311-3.
- Hui Zou and Trevor Hastie. Regularization and variable selection via the elastic net. *J. R. Statist. Soc. B*, 67(2):301–320, 2005.
- Franck Ramus. Acoustic correlates of linguistic rhythm: Perspectives. In *Proceedings of Speech Prosody 2002*, pages 115–120, 2002. doi:10.1.1.16.326.
- Anastassia Loukina, Greg Kochanski, Burton Rosner, Elinor Keane, and Chilin Shih. Rhythm measures and dimensions of durational variation in speech. *The Journal of the Acoustical Society of America*, 129(5):3258–3270, 2011. ISSN 0001-4966. doi:10.1121/1.3559709.
- Volker Dellwo. Czech Speech Rhythm and the Rhythm Class Hypothesis. *English*, (August):1241–1244, 2007.
- Marina Nespor. On the rhythm parameter in phonology. In *Logical Issues in Language Acquisition*, pages 157–176. De Gruyter Mouton, Berlin, Boston, 1990. ISBN 978-3-11-087037-4. doi:10.1515/9783110870374-009.
- Paolo Mairano. *Rhythm Typology: Acoustic and Perceptive Studies*. PhD thesis, Università degli studi di Torino, March 2011.
- Robert V Shannon, Fan Gang Zeng, Vivek Kamath, John Wyganski, and Michael Ekelid. Speech recognition with primarily temporal cues. *Science*, 270(5234):303–304, 1995. ISSN 00368075. doi:10.1126/science.270.5234.303.
- Klaus J. Kohler. Whither speech rhythm research? *Phonetica*, 66(1-2):5–14, 2009b. ISSN 00318388. doi:10.1159/000208927.
- Francoise Beaufays, Hasim Sak, and Andrew Senior. Long Short-Term Memory Recurrent Neural Network Architectures for Large Scale Acoustic Modeling Has. *Interspeech*, (September):338–342, 2014. ISSN 0028-0836. doi:arXiv:1402.1128.
- Andrej Karpathy, Justin Johnson, and Li Fei-Fei. Visualizing and understanding recurrent networks. In *ICLR Workshop*, June 2016. ISBN 978-3-319-10589-5. doi:10.1007/978-3-319-10590-1_53.
- Radoslaw M. Cichy and Daniel Kaiser. Deep Neural Networks as Scientific Models. *Trends in Cognitive Sciences*, 23(4): 305–317, April 2019. ISSN 1879307X. doi:10.1016/j.tics.2019.01.009.
- Nick Cammarata, Shan Carter, Gabriel Goh, Chris Olah, Michael Petrov, and Ludwig Schubert. Thread: Circuits. *Distill*, March 2020. ISSN 2476-0757. doi:10.23915/distill.00024.
- F. Ramus and J. Mehler. Language identification with suprasegmental cues: A study based on speech resynthesis. *The Journal of the Acoustical Society of America*, 105(1):512–521, January 1999. ISSN 0001-4966. doi:10.1121/1.424522.
- Jonas Kubilius, Stefania Bracci, and Hans P. Op de Beeck. Deep Neural Networks as a Computational Model for Human Shape Sensitivity. *PLoS Computational Biology*, 12(4):e1004896, April 2016. ISSN 15537358. doi:10.1371/journal.pcbi.1004896.
- Felix A. Wichmann and Robert Geirhos. Are Deep Neural Networks Adequate Behavioral Models of Human Visual Perception? *Annual Review of Vision Science*, 9(1):501–524, 2023. doi:10.1146/annurev-vision-120522-031739.
- Matthew L Leavitt and Ari S Morcos. Towards falsifiable interpretability research. In *NeurIPS 2020, ML-RSA Workshop*, 2020.